



Synthesis and thermo-physical properties of chitosan/poly(DL-lactide-co-glycolide) composites prepared by thermally induced phase separation

Santos Adriana Martel-Estrada^{a,*}, Carlos Alberto Martínez-Pérez^b, José Guadalupe Chacón-Nava^a, Perla Elvia García-Casillas^b, Imelda Olivas-Armendariz^b

^a Centro de Investigación en Materiales Avanzados, Departamento de Física de Materiales, Miguel de Cervantes 120, Complejo Industrial Chihuahua, C.P. 31109, Chihuahua, México, Mexico

^b Instituto de Ingeniería y Tecnología, Universidad Autónoma de Cd. Juárez, Av. Del Charro 450 Norte, Col. Partido Romero, C.P. 32310, Cd. Juárez, Chihuahua, México, Mexico

ARTICLE INFO

Article history:

Received 30 September 2009

Received in revised form 6 January 2010

Accepted 19 March 2010

Available online 25 March 2010

Keywords:

Chitosan

Poly(DL-lactide-co-glycolide)

Scaffold

Thermal properties

Thermally induced phase separation

ABSTRACT

Chitosan and poly(DL-lactide-co-glycolide) (DLPLG) were used to fabricate biodegradable porous scaffolds for applications in tissue engineering by thermally induced phase separation (TIPS) technique. Parameters such as polymer concentration, quenching temperature, solvent ratio and different compositions were analyzed. Aqueous glacial acetic acid solution was used as a solvent for chitosan and chloroform for the lactide part. Through the use of a field emission scanning electron microscopy, the variation in porous morphology was studied. The cumulative results obtained from IR and X-ray diffraction spectra, TGA, DSC and DMA suggest that there is a chemical interaction between the components of the composite.

© 2010 Elsevier Ltd. All rights reserved.

1. Introduction

Polymeric composites that mimic the structure and function of the natural extracellular matrix (ECM) are of great interest in tissue engineering. This kind of materials can be used as scaffolds that restore, maintain or improve the function in tissues or organs (Bhattacharai, Edmondson, Veiseh, Matsen, & Zhang, 2005). Biodegradable polymers are of the most promising materials to restore tissue (Duan et al., 2006). These materials have to provide a suitable environment for the adherence, proliferation and differentiation of cells. The scaffold should meet the following requirements for a successful biological application: biocompatibility with the living organism, well controlled biodegradability, non-toxicity and non-antigenic, adequate mechanical properties and morphology for cells transporting, gases, metabolites, nutrients within the scaffold and the local environment (Kim et al., 2008).

Poly(DL-lactide) (PLA) has been used in tissue engineering due to its properties such as biodegradability, biocompatibility, good mechanical properties and its ability to be dissolved in common solvents. The biodegradability rate can also be controlled

using substances with similar structure but faster degradation than PLA, for example, glycolide, producing a copolymer called poly(DL-lactide-co-glycolide) (DLPLG). Similarly, chitosan has been considered to be one of the most promising biopolymers due to the fact that it is biologically renewable, biodegradable, biocompatible, antibacterial, non-antigenic and possess a wound healing quality (Bhattacharai et al., 2005; Duan et al., 2006; Kim et al., 2008). It is a copolymer of (1→4)-2-acetamido-2-deoxy-β-D-glucan(N-acetyl-D-glucosamine) and (1→4)-2-amino-2-deoxy-β-D-glucan (D-glucosamine) units randomly or block distributed throughout the polymer chain depending on the processing method in which it was obtained (Thein-Han & Misra, 2009). Due to its solubility properties, in order to prepare a solution it is essential, to use acidic organic solvents such as acetic acid or formic acid. Most polymers, especially synthetic ones can only be dissolved in non-acidic organic solvents. As a result the choice of solvents to prepare blends containing chitosan is limited (Han, Liu, & Bai, 2007). In order to dissolve both polymers in a blend, a solution of DLPLG in chloroform was dropped slowly in chitosan previously dissolved in an acetic acid aqueous solution. In earlier studies developed by other research groups, methodologies to synthesize chitosan with different polymers through freezing and lyophilization, step-wise co-precipitation, electrospinning, and so on were described. In this work the preparation of chitosan–DLPLG by thermal induced

* Corresponding author. Tel.: +52 656 688 48 87; fax: +52 656 688 48 13.
E-mail address: adriana.martel@cimav.edu.mx (S.A. Martel-Estrada).

phase separation is described. To the best of our knowledge, the preparation solely by this method, has not been reported for this kind of composites as of yet. Therefore, in this work, the synthesis, morphology, FTIR and X-ray diffraction spectra and thermal characterization of these composites are described.

2. Materials and methods

2.1. Materials

Chitosan was purchased from Carbomer Inc. (United States). 75:25 poly(DL-lactide-co-glycolide) with an inherent viscosity range of 0.55–0.75 dK/g in CHCl_3 was purchased from Lactel (United States). Ethanol and chloroform (CTR Scientific Mexico) and glacial acetic acid (Mallinckrodt, United States) were used as solvents.

2.2. Preparation of the composites

Chitosan/dLPLG composites with different compositions, 70/30, 50/50 and 30/70 were prepared by the following procedure. Typically, 5% (%w/v) dLPLG in chloroform was added to a 2 wt% of chitosan in a glacial acetic solution (0.1 M) at a rate of 1 drop/min, approximately. After the dLPLG solution was completely added to the chitosan solution, the solution was stirred for 1 h followed by 10 min of sonification in order to eliminate the gas from the gelatinous mixture. Following this process, each composite was frozen at -78°C for 3 h or 6 h. The solvent was then extracted by a freeze drying system Labconco FreeZone 2.5. The composites were neutralized by immersion in ethanol at -20°C during 12 h followed by another 12 h immersion into $\text{NaOH}-\text{CH}_3\text{CH}_2\text{OH}$ aqueous solution (prepared using an 80% ethanol aqueous solution mixed previously with 0.5 (w/w%) of NaOH) at the same temperature. Then the samples were washed and rinsed with distilled water 5 times.

2.3. Characterization of the samples

In order to make the chemical characterization of the composites FTIR-ATR spectrometer Nicolet 6700 was used. Each dried sample was used without any special preparation for the FTIR scan. All spectra were recorded using 100 scans and 16 cm^{-1} resolution. The X-ray diffraction patterns of the samples were analyzed between $2\theta = 5^\circ$ and $2\theta = 80^\circ$ with a step size of $2\theta = 0.02^\circ$ in an X-ray diffraction instrument in continuous mode (PANanalytical X'Pert PRO). The morphology characterization was made in a Field Emission Scanning Electron Microscope JEOL JSM-7000F; the samples were dried previously for 3 days at room temperature in a vacuum oven (-677 mbar). The average pore size and the pore size distribution were measured using the Scandium Universal SEM Imaging Platform software (Soft Imaging System) from the SEM micrographs in the original magnification. Three different cross-sections of each scaffold were used to estimate the pore size and at least 120 pores to estimate the distribution. The dried composites were frozen in liquid nitrogen and then cut in small pieces ($5\text{ mm} \times 5\text{ mm} \times 10\text{ mm}$) with a blade to get a cross-section for SEM analysis. The electric voltage was controlled at 1.0 kV.

The porosity was determined by measuring the scaffold density in a graduated cylinder. Ethanol with density ρ_e at -20°C was used as the displacement liquid. A sample with volume V_t and weight w_s was immersed in ethanol at -20°C for 20 min at the same temperature. After that, the wet sample was taken and the final weight was registered as w_{se} . The porosity was calculated using Eq. (1):

$$\text{Porosity\%} = \frac{w_{se} - w_s}{\rho_e V_t} \quad (1)$$

2.4. Thermal analysis

Thermogravimetric analysis (TGA) of chitosan/dLPLG composites was carried on SDT Q600 from TA Instruments (United States). The dry samples were heated from room temperature to 750°C at $5^\circ\text{C}/\text{min}$ under nitrogen atmosphere with a flow rate of $160\text{ mL}/\text{min}$. The first derivative of the mass-change with respect to time (DTG) was calculated and plotted as a function of the temperature. Differential Scanning Calorimetric (DSC) measurements were carried out on Netzsch DSC 200 PC (Germany). In order to erase the thermal history of the samples they were heated from room temperature to 260°C at $20^\circ\text{C}/\text{min}$. Then, they were cooled from 260°C to -20°C at the same rate of $20^\circ\text{C}/\text{min}$. Finally, they were heated from -20°C to 260°C at $10^\circ\text{C}/\text{min}$ under a nitrogen atmosphere. RSA III (Rheometrics Analyzes System) TA was used to make a dynamic temperature ramp test in a frequency of 6.2832 rad/s and in a temperature range of $35.0\text{--}300^\circ\text{C}$, for all samples, excepting dLPLG. Disks of approximately 5 mm in thickness and 15 mm in diameter were used in all the experiments. Samples were mounted in a compression clamp.

3. Results and discussion

3.1. FTIR analysis

When two substances are mixed, it is possible to compare if a physical mix or a chemical interaction was produced, analyzing the changes in the characteristic peaks of the substance in an IR spectrum (Bourtoom & Chinnan, 2008; Choi et al., 2008; Jevtic, Radulovic, Ignjatovic, Mitric, & Uskokovic, 2009; Li, Jiang, Huang, Ding, & Chen, 2008; Sokker, Ghaffar, Gad, & Aly, 2008; Sutton, Durand, Shuai, & Gao, 2006). These changes could result in the appearance of new peaks or shifts of existing peaks (Liu & Bai, 2005).

In Fig. 1, the IR spectra of the materials are shown, the chitosan spectrum shows the characteristic bands at 1574 cm^{-1} which can be assigned to N–H bending vibration (amide II). The peak at 1644 cm^{-1} corresponds to the stretching $\text{C}=\text{O}$ (amide I), and the peak at 1409 cm^{-1} appeared to $\text{C}-\text{O}$ stretching of primary alcoholic group in chitosan. The band at 1034 cm^{-1} suggests the presence of an ether group. The spectrum also shows peaks at 1151 cm^{-1} and 896 cm^{-1} that could be attributed to the saccharide structure.

The dLPLG IR spectrum shows the main bands of this copolymer at 3000 cm^{-1} , 2932 cm^{-1} and 2851 cm^{-1} that corresponds to the bond $\text{C}-\text{H } \nu_1$, while the peaks at 749 cm^{-1} and 671 cm^{-1} are attributed to the vibrations $\text{C}-\text{H } \nu_2$. Another intense band is located at 1756 cm^{-1} that corresponds to the $\text{C}=\text{O}$ of DL-lactide. Also, the bands at 1448 cm^{-1} , 1415 cm^{-1} and 1376 cm^{-1} are attributed to the vibrations of the group CH_3 , the first and second correspond to the asymmetric CH_3 and the last one to the symmetric CH_3 of PLGA. The absorption peaks for the $\text{C}-\text{O}$ stretching vibrations of PLGA are located at 1263 cm^{-1} , 1187 cm^{-1} and 1092 cm^{-1} .

The N–H band was affected and shifted from 1574 cm^{-1} to 1558 cm^{-1} , 1556 cm^{-1} and 1541 cm^{-1} , respectively for 70/30, 50/50 and 30/70 composites. The peak that corresponds to the primary alcohol groups ($\text{C}-\text{O}$ stretching) was shifted from 1409 cm^{-1} to 1419 cm^{-1} , 1420 cm^{-1} and 1422 cm^{-1} for the composites 70/30, 50/50 and 30/70 respectively. Furthermore, it is possible to observe a more pronounced peak in the spectrum of 70/30 composite at 2915 cm^{-1} , corresponding to the $\text{C}-\text{H}$ stretching of chitosan than in the other composites (30/70 at 2947 cm^{-1} and 50/50 at 2938 cm^{-1}) that could be overlapped with the $\text{C}-\text{H } \nu_1$ of dLPLG. The spectrum of 50/50 composite shows a reduced intensity on the band at 1039 cm^{-1} while the 30/70 composite does not show this band. This could imply that an interaction of the ether bond of chitosan with the poly(DL-lactide-co-glycolide) occurred. The spectrum of

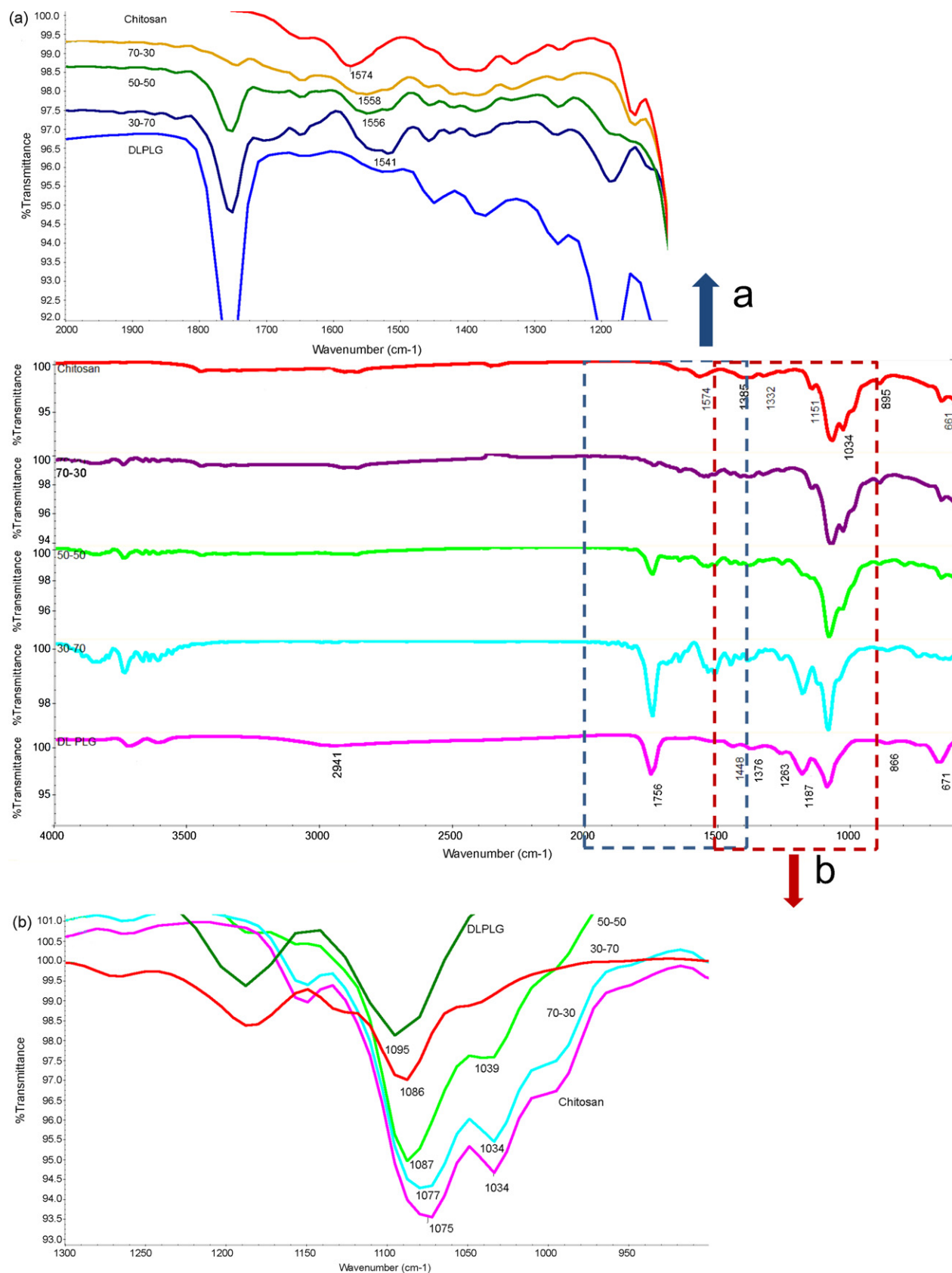


Fig. 1. IR spectra of chitosan, DLPLG and 70/30, 50/50 and 30/70 Ch/dLPLG composites.

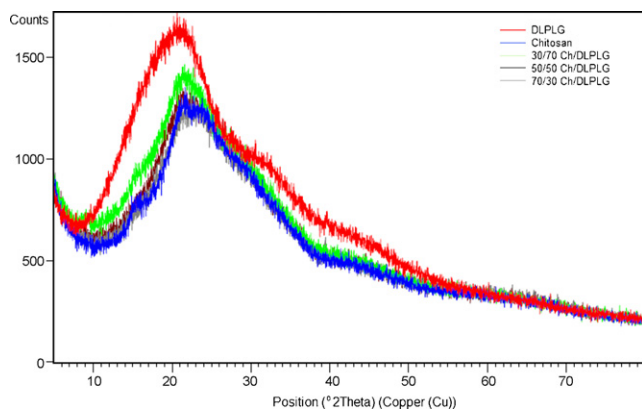


Fig. 2. X-ray diffraction pattern of chitosan, DLPLG and the composites.

30/70 composite shows a band between 1435 cm^{-1} and 1403 cm^{-1} corresponding to the CH_3 bonds of poly(DL-lactide-co-glycolide). This spectrum also shows a pronounced band at 1756 cm^{-1} that corresponds to $\text{C}=\text{O}$ bond of the poly(DL-lactide-co-glycolide), but shifted slightly to the left and with a reduced intensity for the 70/30 (1745 cm^{-1}), 50/50 (1752 cm^{-1}) and 30/70 (1752 cm^{-1}). All these events suggest that there is an interaction between the amino group of the chitosan and carboxyl groups in DLPLG or hydroxyl groups in chitosan and carboxyl groups of the DLPLG in the blend.

Similar results were reported by Wan, Wu, Yu, and Wen (2006) and Wan, Fang, Wu, and Cao (2006) and Niu, Feng, Wang, Gui, and Zheng (2009) in their study of poly(lactic acid)/chitosan and poly-lactide/chitosan, respectively. During their research, they found that the existence of hydrogen bonds formed between amino groups of chitosan and carboxyl groups of DLPLG or hydroxyl groups of chitosan and carboxyl groups of DLPLG might be possible.

3.2. X-ray diffraction

Fig. 2 shows XRD pattern of chitosan, DLPLG and the composites. The pure chitosan sample is amorphous with a halo that peaks around $2\theta = 21.70^\circ$. This peak is in agreement with other published results (Majd, Yuan, Mishra, Haggard, & Burngardner, *in press*; Souza et al., *in press*). The reflection at 20° corresponds to the regular crystal lattice (1 1 0) of chitosan (Souza et al., *in press*). Also, it has been reported that the dissolution of chitosan in acetic acid causes a decrease in its crystallinity (Schiffman et al., *in press*), and maybe it is the cause of the low crystallinity shown.

As it has been reported in the literature, the poly(DL-lactide-co-glycolide) is amorphous (Kang et al., 2008). During this research, it shows a halo pattern with a broad peak between 10° and 40° . When the lactide is added to the chitosan, the chitosan peak decreased resulting in completely amorphous composites. The XRD results suggest that there were good compatibility and interaction between chitosan and lactide in the composite. The interaction causes the decreasing of crystallinity of chitosan, due to the incorporation of amorphous lactide into it, suggesting a hydrogen

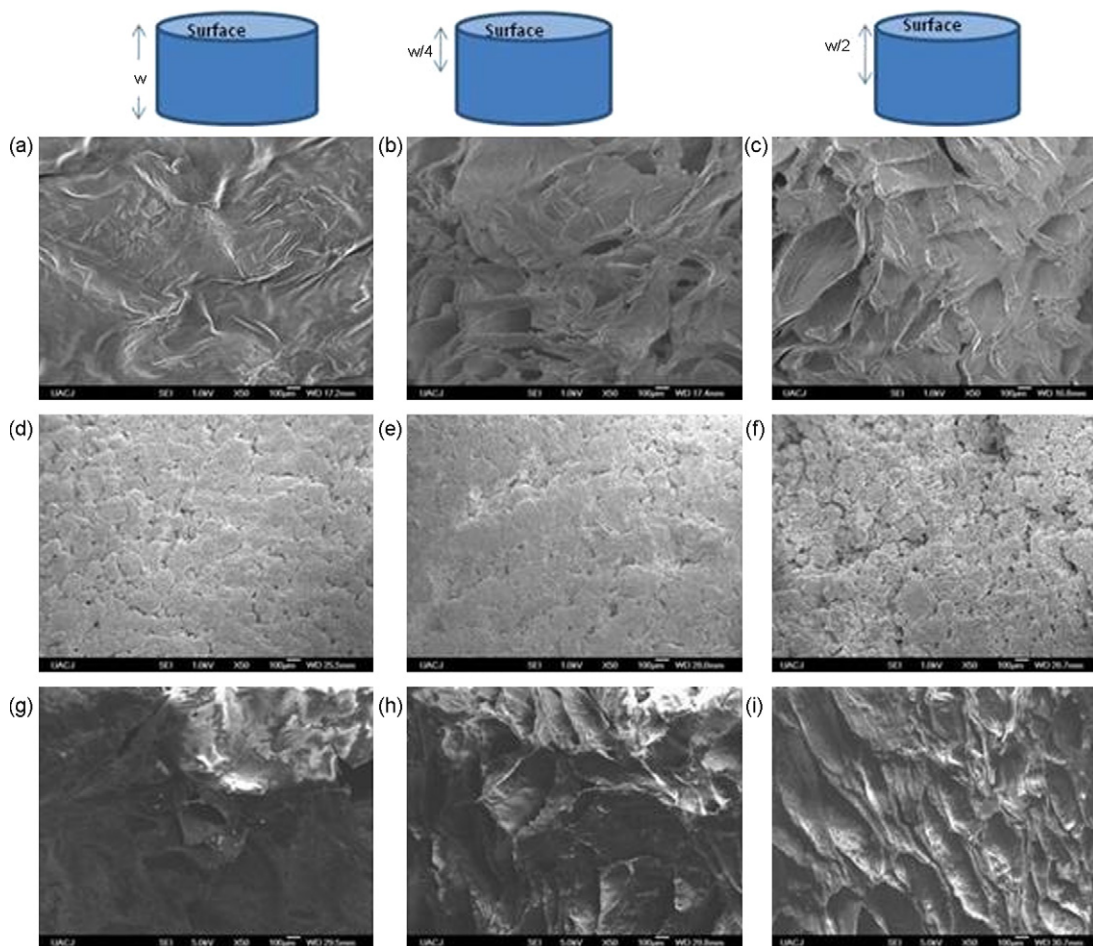


Fig. 3. SEM micrographs of (a–c) chitosan, (d–f) 30–70 (g–i) 70–30 with different cross-sections; that is, at the surface, $w/4$ and $w/2$, where w is the width of the liophilized scaffold after neutralization.

bonding between them which leads to their good compatibility (Nagahama et al., 2009).

3.3. Characterization of the morphology

In Fig. 3, the morphology of the composites is shown where a porous structure can be appreciated, the lyophilized and neutralized composites present a porous structure mainly in deep planes of the scaffold and smaller porous at the surface. A higher magnification shows that inside the big porous structure of the composites exists a highly interconnected porous structure ($<10\text{ }\mu\text{m}$ porous). The mesopores are important to provide an environment that stabilizes enzyme activities for long periods of time (Cooney et al., 2008). At least 20% of the pores should be smaller than $20\text{ }\mu\text{m}$, because porous structures with less than $1\text{ }\mu\text{m}$ of size are important to interact with proteins and bioactivity, and porous structures between $1\text{ }\mu\text{m}$ and $20\text{ }\mu\text{m}$ for cellular development, type of cells attracted and orientation and directionality of the cellular ingrowth (Sánchez-Salcedo, Nieto, & Vallet-Regí, 2008). Fig. 4 shows this kind of inner porosity in 70/30 and 30/70 composites. Although other research tried to combine chitosan and a lactide in a blend, the morphology showed a visible microscopically phase separation between them, showing a great number of dispersed small balls of lactide embedded into a continuous chitosan matrix (Wan, Wu, et al., 2006; Wan, Fang, et al., 2006). In our work there is not a visible phase separation getting a well blend between the lactide and chitosan.

The process conditions were elemental to control the phase separation. Also, the freezing temperature will define the pore size. Chitosan solutions of 0.5–2.0 wt% can be easily prepared by using 1.0% (v/v) glacial acetic acid aqueous solutions and frozen in a broad range of temperatures of at least $-10\text{ }^{\circ}\text{C}$. However, when chitosan is blending with DLPLG –chloroform solution, the freezing temperature is restricted. Firstly, the samples cannot be frozen using temperatures higher than $-70\text{ }^{\circ}\text{C}$ due to the combination of concentrations and the melting point of chloroform ($-63.5\text{ }^{\circ}\text{C}$). Secondly, if the blend was not frozen immediately after it is prepared, then the components would be likely to precipitate out of the mixture during the frozen process. For these reasons, dry ice was used to overcome these problems. During the experiments, liquid nitrogen was also used to analyze the effect of low temperatures on porosity. Nevertheless, due to the polymer concentration, the process was in a metastable region of low polymer concentration, and droplets of polymer-rich phase were formed and dispersed in a matrix of polymer-lean phase and the resulting structure after removing the solvent was a micro-spheres-like polymer solid. Consequently, it was not possible to control the porosity through temperature.

The morphology of scaffolds, depends upon the route in which the phase separation between the solvents and polymers takes place. In our system, under the described conditions, it was a

liquid–solid phase separation. Chloroform is miscible in acetic acid but not in water. In the mixture the major content corresponds to water, so it is possible that water can have a great influence on the crystals shape. While the chloroform and acetic acid could mix, at freezing temperatures the water separates from the chitosan forming crystals where the polymer could precipitate. During the experiments, we observed that the acetic acid–water–chloroform–polymers solution has a higher melting point than the DLPLG –chloroform solution, because the composites can be frozen at $-78\text{ }^{\circ}\text{C}$ while the lactide–chloroform solution cannot. Also, the acetic acid acts as a freezing point depressant of water, therefore the water–acetic acid solution freezing point, temperature gradient and rate of ice crystal growth are lowered (Cooney et al., 2008). The form of the crystals will define the kind of porosity and the pore size obtained; that is, the inner porous structure will be similar to the geometry of the water crystals after they were totally sublimated. In order to understand how the crystals are grown, it is very important to define the dominant thermal separation process. That is, if the process is dominated by mass or heat transfer. It has been reported that below $-50\text{ }^{\circ}\text{C}$ the dominant process for aqueous systems of chitosan is heat transfer (Cooney et al., 2008; Roh & Kwon, 2002). The main difference between these processes is related to what kind of porosity is produced. When the dominant process is mass transfer, diffusional processes define the crystals growth, so the growth is directionally homogeneous and the crystals shape will be spherical. On the other hand, when dominant process is heat transfer the thermal gradient is larger, and if it is directional, the diffusion rate of the water molecules to the ice crystals will be greater in the direction of the thermal gradients. Nevertheless, as is shown in Fig. 3h, the porosity could be reached, but elongated in the direction of the thermal gradient.

We also found that the thermal gradient affects the size of crystals from the surface to the inner part of the composite. Usually, the crystals grow from the surface to the center. This idea was proved, measuring the pore size at different depths from the surface to the center. It was found to be more uniform and contain a larger pore size inside the composite than in the surface as shown in Fig. 3 for chitosan and 70–30 and 30–70 composites.

Also, in this study, the temperature gradient induced was relatively large because the blends were fabricated at $40\text{ }^{\circ}\text{C}$ approximately, and after the gelation point, they were frozen to $-78\text{ }^{\circ}\text{C}$ (dry ice) in few minutes. As a result, the crystals size was small, because the cooling rate is inversely related to the pore size obtained. Faster cooling rates tend to produce smaller crystals because there is not sufficient time for large particles to form (Hsieh et al., 2007; Yuan et al., 2009).

The pore size and pore distribution was calculated from the SEM images by the use of Scandium Universal SEM Imaging Platform software (Soft Imaging System). Table 1 shows those ranges for the developed composites.

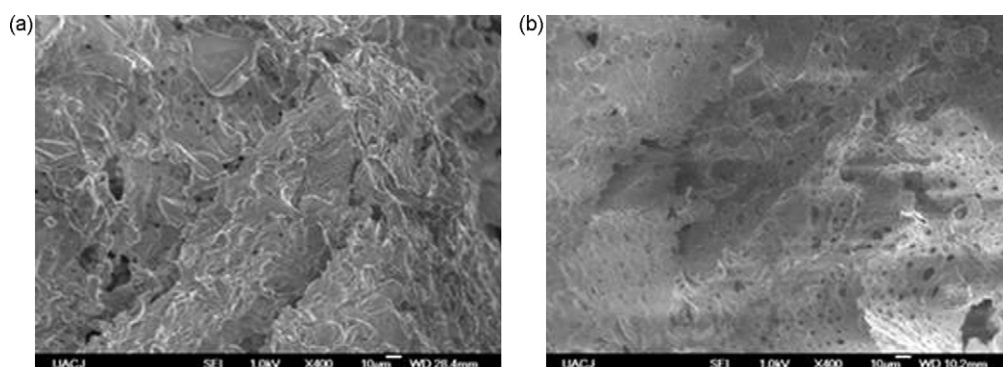
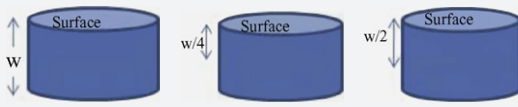


Fig. 4. Porosity of (a) 70/30 y (b) 30/70 composites.

Table 1
Pore size, porosity and pore distribution for the chitosan/dLPLG composites.

Composite (Ch/dLPLG)	Pore size range (μm)			Porosity	Pore size distribution					
					<1 (μm)	1–5 (μm)	5–10 (μm)	10–50 (μm)	50–100 (μm)	>100 (μm)
Chitosan	–	0.48–506.03	1.45–279.24	81%	0.00%	13.11%	9.84%	28.69%	15.57%	32.79%
70/30	0.04–35.55	0.64–317.13	0.53–188.85	68%	28.23%	39.52%	5.32%	5.32%	5.32%	39.52%
50/50	0.64–57.97	0.70–573.20	0.47–517.95	7%	13.33%	3.33%	4.67%	22.00%	12.00%	10.67%
30/70	0.45–64.68	0.33–188.72	0.71–249.24	88%	10.59%	33.53%	2.35%	36.47%	33.53%	2.35%

An agreement does not exist regarding the optimum pore size for the use in different tissue engineering applications; the size depends on the specific cells in which the scaffold will be used, some researchers found success in cultures with pore sizes in the ranges $121.84 \pm 23.44 \mu\text{m}$ (Lee, Lim, Lee, Atala, & Yoo, 2006) and $60\text{--}150 \mu\text{m}$ (Hua et al., 2004) for osteoblasts. On the other hand, for applications in articular cartilage it was used a pore size between $20 \mu\text{m}$ and $500 \mu\text{m}$ (Kawanishi et al., 2004). In this context, according to the results, the 50/50 composite shows the higher pore size, even in the range that has been used for this last kind of tissue. Furthermore, the range of pore size of the all developed composites could be appropriate for vascularization process of cells like fibroblasts and chondrocytes according with their size.

The percentage of porosity of the scaffolds is a key factor for the use of the composites in tissue engineering. In order to get more information about it, the frozen time and temperature (6 h and -78.5°C) and the chitosan concentration in acetic acid solution at 2% were fit. Then, 5% of dLPLG concentration in chloroform was used. The results of porosity and pore size distribution are also shown in Table 1. It could be observed that, although the 30/70 composite had a small pore size, it had a higher porosity percentage than the other composites. These results could imply that small crystals of chloroform form in the matrix during the freezing process that are sublimated during liophilization. This suggests that it is possible for water to be the main cause for larger porosity, while the chloroform only produces small porosity.

3.4. Thermal analysis

To assess the thermal properties of the composites, TGA analysis was performed. In general, chitosan will decompose before melting. The chitosan was thermally decomposed in the region of 232°C and 326°C as shown in Fig. 5. This thermal decomposition could be attributed to a complex process including the dehydration of the

saccharide rings and followed decomposition of chitosan backbone (Lewandowska, 2009).

dLPLG was 100% decomposed in the region of $272\text{--}331^\circ\text{C}$. With respect to the composites thermal behavior, the region and percentage of decomposition is shown in Table 2. In general, as the percentage of chitosan increases, the thermal stability of the composites increases as well, although the thermal stability of the composites in almost all cases was reduced compared with the main substances, both chitosan and dLPLG. Nevertheless, the range of decomposition temperatures is similar in almost all cases, except in the 30/70 composite where the initial and final temperatures of decomposition were reduced at least by 25°C .

There are two stages of degradation in the TGA curve of all samples. The initial weight loss of the composites ($100\text{--}150^\circ\text{C}$) is due to evaporation of the absorbed moisture. This loss depends on the initial moisture content of the composites. The hydrophilic nature of chitosan is important to determine the thermal behavior of the composites. In fact, it is possible to observe the tendency to increase weight loss, with an increase of chitosan content during this stage. The second stage, is the severe weight loss that is called main region of decomposition in Table 2. It is due to the decomposition of the major components of the composites. In order to examine the plots, the weight loss percentage of all samples was differentiated and the derived data are depicted in Table 2. The T_{max} corresponds to the temperature at the maximum degradation rate. All composites exhibit a single peak of fast thermal degradation. It is clear that there are differences existing in these data. In accordance with some researchers (Lewandowska, 2009), an improved thermal stability would be achieved for the component with the lower T_{max} if the measured T_{max} shifts to the higher T_{max} of another component due to the chemical interactions between the substances. Nevertheless, it is clear that the T_{max} of chitosan and dLPLG are similar, as a consequence the combinations that enhance the thermal stability in the composites are 70/30 and 50/50. Furthermore, the onset of degradation temperatures supports this idea. The onset temperatures are almost the same in chitosan and dLPLG, so it was not possible to observe an improvement in a measurable way of the thermal properties of the composites. The onset temperatures and T_{max} of the composite 30–70 is the more affected by the interaction between chitosan and dLPLG. This result suggests that the acid release during the degradation of lactide part of dLPLG influences the degradation of chitosan. It has been reported that at higher temperatures poly(glycolide) degrades, increasing the proportion of carbon dioxide and formaldehyde, so the chain end scission of the polymer increase. Also poly(dL-lactide), changes its degradation rates during dynamic heating, releasing acid that could influence the degradation of other polymers in a composite (Sivalingam & Madras, 2004).

The DTG profiles (Fig. 6) show that the Ch and dLPLG composites have only single peak for all composites, indicating that the chemical interaction between chitosan and dLPLG resulted in a relatively homogenous composition of the chitosan/dLPLG composites as is

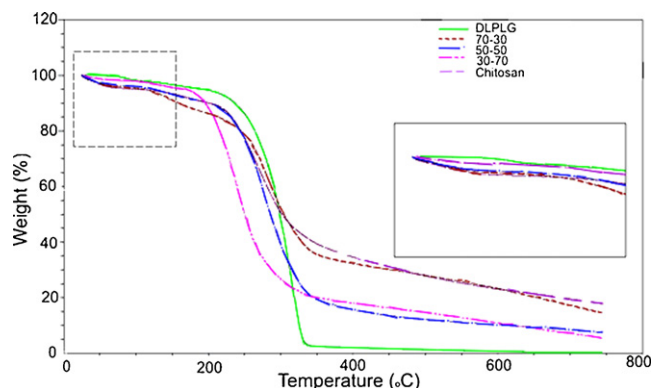


Fig. 5. Thermal decomposition of chitosan, dLPLG and 70/30, 50/50 and 30/70 composites.

Table 2

Region and percentage of decomposition weight of the composites.

Composites (Ch/dLPLG)	Main region of decomposition (°C)	Percentage of decomposition weight	T_{\max} (°C)	Maximum degradation rate (%/min)	Onset Degradation Temperature (°C)
Chitosan	232–326	80.55%	271.35	2.771	327.18
70/30	242–317	84.21%	284.19	2.965	317.76
50/50	227–374	96.29%	278.11	2.676	324.03
30/70	202–278	93.90%	239.32	4.844	278.54
dLPLG	272–331	100%	308.52	6.858	331.16

shown in Fig. 6. Nevertheless, due to the limitations of TGA, other techniques such as DSC could help to define if there is an existence of more than one Tg for each composites in order to figure out if both substances are miscible or not.

It is known that the observation of the glass transition temperature Tg for a blend, is used as a criteria to define the composite components miscibility. When two components in a composite are well blended together and completely miscible between them, only one new Tg must be observed between the original Tgs of components in the DSC curve. On the contrary, if the components are partially miscible, the resulting blends would have two Tgs

related to each component, although the Tgs value could be affected depending on the composition ratios (Lewandowska, 2009). The DCS curves obtained for the composites are presented in Fig. 7f.

Chitosan is a semi-crystalline polymer due to its strong inter- and intra-molecular hydrogen bonds. This is the reason why it is difficult to find its Tg through DSC method, although it was possible to find the Tg of dLPLG and the composites chitosan/dLPLG. The Tg was 45.2 °C, 40.7 °C, 39.8 °C and 31.6 °C for dLPLG, 30/70, 50/50 and 70/30 composites respectively. As it can be seen, the Tg moved to a lower value as the percentage of chitosan is increased. Also, it could be observed that dLPLG is amorphous, so no endothermic peak can be seen. Due to the fact that these results are only evidence of a partial miscibility between the composite components, a more sensitive method such as dynamical mechanical analysis could be employed.

DMA is a useful instrument to complement investigations of thermal properties of polymeric composites (Liu et al., 2004) and it is a sensitive technique to investigate relaxation processes in relation to the molecular motions associated with internal changes in a polymer composite (Wan, Wu, et al., 2006; Wan, Fang, et al., 2006). Also, the use of this technique makes possible to analyze the $\tan \delta$ curve. Generally, for a highly miscible blend, the curves show only a single peak in between the transition temperatures of the components. In the case of miscible or partially miscible blends the Tgs change as a function of composition (Perera, Ishiaku, & Ishak, 2000). Fig. 7a–e, illustrates the temperature dependence of the storage modulus (E') and the damping tangent ($\tan \delta$) for the composites. It is known that the plots of $\tan \delta$ could be used to measure the characteristic temperatures related with relaxation processes (Wan, Wu, et al., 2006; Wan, Fang, et al., 2006). The dLPLG exhibited a noticeable drop in storage module since the initial part of the test, while the composites reduced them around 60 °C. The Tg of dLPLG was found at 54 °C. This result is in agreement with the thermal–mechanical behavior of this material found in other researches (Liu et al., 2004), where it was tested using a broad temperature range and showed a sharp glass transition and above this temperature the sample no longer gave any force readings on the instrument. In our study, the sample showed valid force readings until approximately 100 °C. Nevertheless, above the glass transition, the chitosan seems to enable the matrix to maintain some level of physical integrity and improve the Tg of the samples.

The change in heat capacity for the chitosan molecules might be small, because the chitosan consist of glucosamine residues, so the DSC results can be confused. Through the use of DMA, two peaks were detected for chitosan samples at 153 °C and 280 °C. It is presumed that chitosan has two relaxations on the $\tan \delta$ of the dynamic mechanical spectra. One of these relaxations is around 100 °C and corresponds to β -relaxation that could be caused by partial acetamide groups attached to the C-2 position in the chitosan backbone (Wan, Wu, et al., 2006; Wan, Fang, et al., 2006). The other peak should be higher than 200 °C and corresponds to the α -relaxation, or Tg of chitosan (Sakurai, Maegawa, & Takahashi, 2000). The glass transition is described as a decrease in storage modulus caused by the decrease in resistance of the material to deformation and a peak in the damping component ($\tan \delta$) due to the increased loss of energy as heat during the transition process

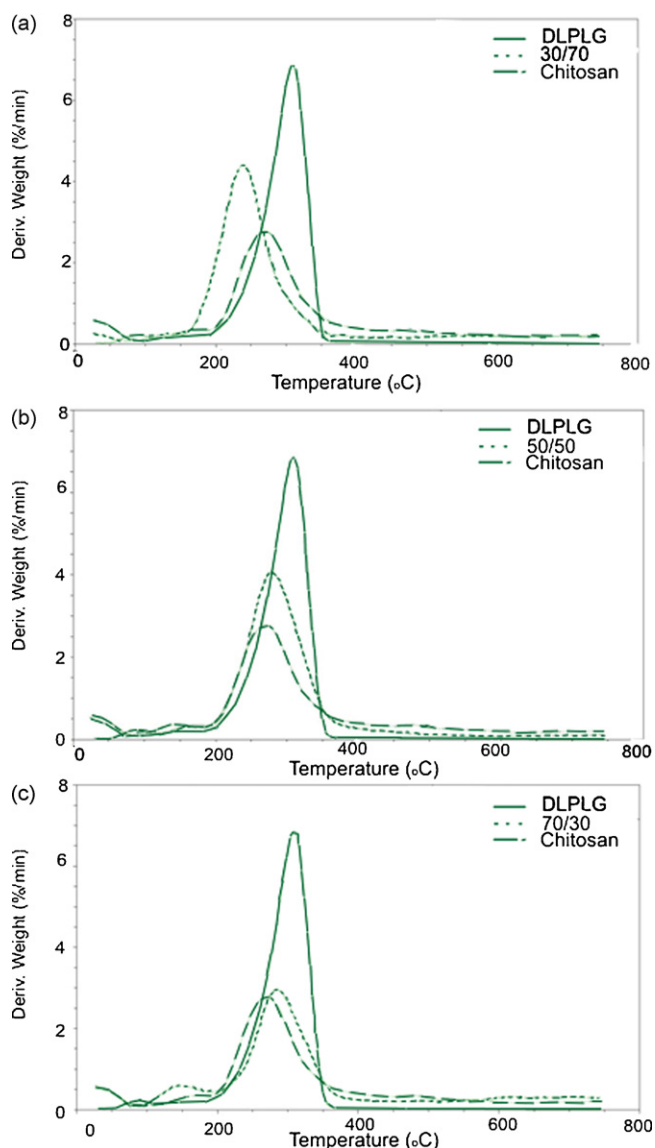


Fig. 6. DTG profiles for composites (a) 30/70, (b) 50/50 and (c) 70/30 chitosan/dLPLG composites.

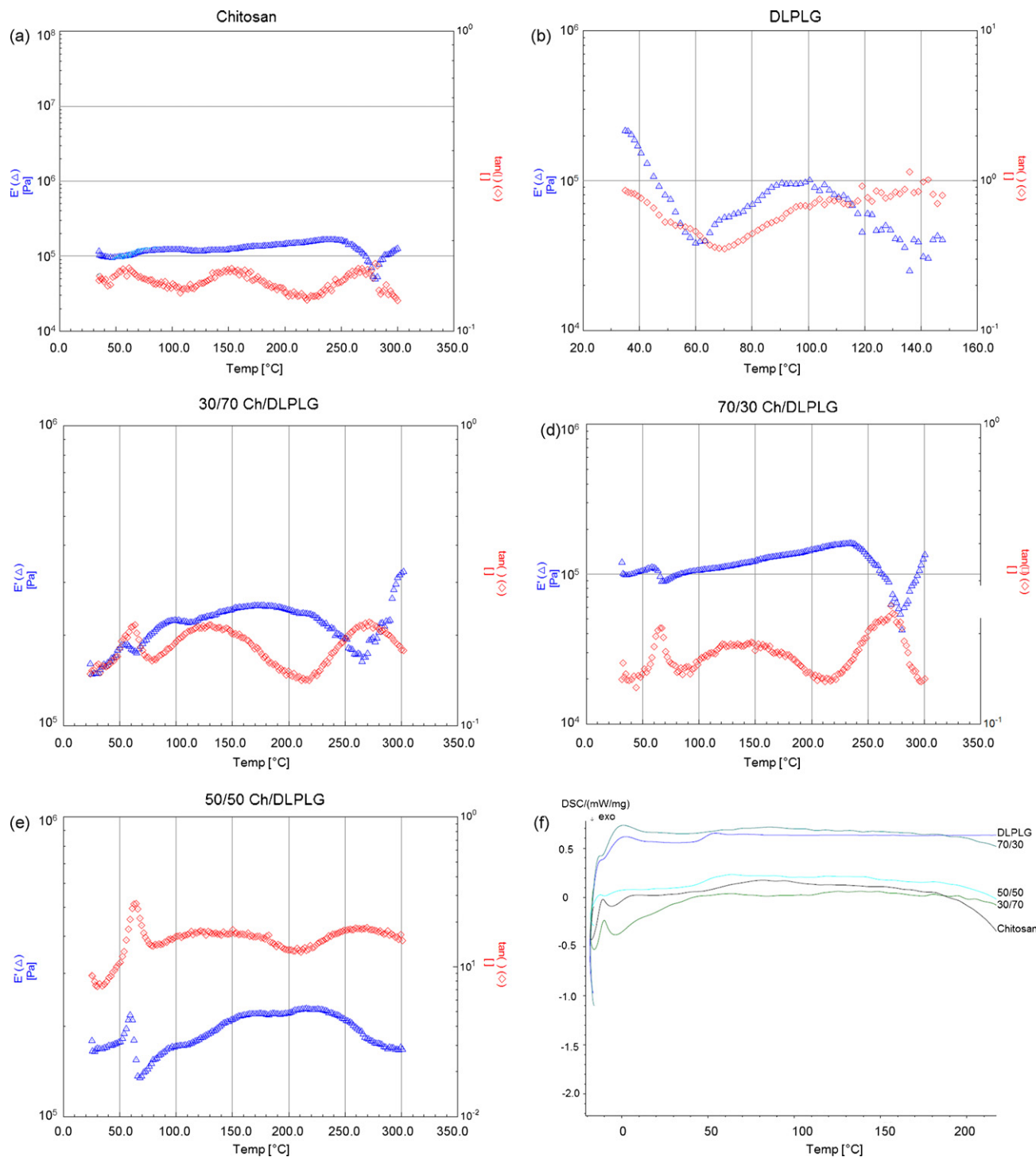


Fig. 7. DMA curves for (a) chitosan, (b) dLPLG, (c) 30/70 Ch/dLPLG, (d) 70/30 Ch/dLPLG, (e) 50/50 Ch/dLPLG and (f) DSC curves for the composites and the main substances.

(Royall et al., 2005), so the peak detected at 280 °C must be the Tg of chitosan.

A similar behavior was also observed for the Ch/dLPLG composites. The relaxation processes found were 63–131–272 °C, 67–146–271 °C and 65–150–270 °C, for 30/70, 50/50 and 70/30 composites respectively. The first temperature is related to the Tg of dLPLG, the second one to the β -relaxation and the last one to the Tg of chitosan. Although the composites did not exhibit any visible phase separation during the preparation procedure, the two Tgs reveal the fact that there are interactions between both components probably from hydrogen bonds, and indicating that these

two components are partially miscible (Wan, Wu, et al., 2006; Wan, Fang, et al., 2006), as it was suggested also for the DSC results. As a conclusion, according to the results and thermal analysis methods used, it is possible to say that evidence shows that a partial miscibility exists between the composites components.

4. Conclusion

Biodegradable chitosan/dLPLG composites have been successfully prepared through a thermally induced phase separation process. A porous morphology that could be appropriated for vas-

cularization process of cells like fibroblasts and chondrocytes was found. The obtained results from IR, X-ray diffraction, TGA, DSC and DMA suggest a chemical interaction between the polymers; and it is believed that an interaction occurred between the amino group (mainly in chitosan) and carboxyl groups in Δ LPLG or hydroxyl (mainly in chitosan) and carboxyl groups in the blends.

Acknowledgements

This study was supported by the Mexican Public Education Secretary and the Mexican National Council for Science and Technology (CONACyT) through project SEP-CONACyT 2007-84339. Authors also thank the support of Monica Mendoza-Duarte, Christian Chapa and Francisco Álvarez-Castrejón during the thermo-mechanical and SEM characterization, and language edition of this document.

References

- Bhattacharai, N., Edmondson, D., Veis, O., Matsen, F., & Zhang, M. (2005). Electrospun chitosan-based nanofibers and their cellular compatibility. *Biomaterials*, 26, 6176–6184.
- Bourtoom, T., & Chinnann, M. (2008). Preparation and properties of rice starch–chitosan blend biodegradable film. *LWT-Food Science and Technology*, 41, 1633–1641.
- Cooney, M., Lau, C., Windmeisser, M., Yann Liaw, B., Klotzbach, T., & Menteer, S. (2008). Design of chitosan gel pore structure: towards enzyme catalyzed flow-through electrodes. *Journal of Materials Chemistry*, 18, 667–674.
- Choi, Y., Kim, M., Kang, H., Park, H., Noh, I., & Park, K. (2008). Evaluation of porous poly(lactide-co-glycolide) scaffold surface-modified by irradiation of nitrogen ion beams. *Surface & coatings technology*, 202, 5713–5717.
- Duan, B., Yuan, X., Zhu, Y., Zhang, Y., Li, X., Zhang, Y., et al. (2006). A nanofibrous composite membrane of PLGA–chitosan/PVA prepared by electrospinning. *European Polymer Journal*, 42, 2013–2022.
- Han, W., Liu, C., & Bai, R. (2007). A novel method to prepare high chitosan content blend hollow fiber membranes using a non-acidic dope solvent for highly enhanced adsorptive performance. *Journal of membrane science*, 302, 150–159.
- Hsieh, C., Tsai, S., Ho, M., Wang, D., Liu, C., Hsieh, C., et al. (2007). Analysis of freeze-gelation and cross-linking processes for preparing porous chitosan scaffolds. *Carbohydrate Polymers*, 67, 124–132.
- Hua, M., Kuo, P., Hsieh, H., Hsien, T., Hou, L., Lai, J., et al. (2004). Preparation of porous scaffolds by using freeze-extraction and freeze-gelation methods. *Biomaterials*, 25, 129–138.
- Jevtic, M., Radulovic, A., Ignjatovic, Mitric, M., & Uskokovic, D. (2009). Controlled assembly of poly(D,L-lactide-co-glycolide)/hydroxyapatite core-shell nanospheres under ultrasonic irradiation. *Acta biomaterialia*, 5, 208–218.
- Kang, Y., Yin, G., Ouyang, P., Huang, Z., Yao, Y., Liao, X., et al. (2008). Preparation of PLLA/PLGA microparticles using solution enhanced dispersion by supercritical fluids (SEDS). *Carbohydrate polymers*, 76, 255–260.
- Kawanishi, M., Ushida, T., Kaneko, T., Niwa, H., Fukunayashi, T., Nakamura, K., et al. (2004). New type of biodegradable porous scaffolds for tissue-engineered articular cartilage. *Materials Science and Engineering*, 24, 431–435.
- Kim, I., Seo, S., Moon, H., Yoo, M., Park, I., Kim, B., et al. (2008). Chitosan and its derivatives for tissue engineering applications. *Biotechnology Advances*, 26, 1–21.
- Lee, S., Lim, G., Lee, J., Atala, A., & Yoo, J. (2006). In vitro evaluation of a poly(lactide-co-glycolide)–collagen composite scaffold for bone regeneration. *Biomaterials*, 27, 3466–3472.
- Lewandowska, K. (2009). Miscibility and thermal stability of poly(vinyl alcohol)/chitosan mixtures. *Thermochimica Acta*, 493, 42–48.
- Li, G., Jiang, Y., Huang, K., Ding, P., & Chen, J. (2008). Preparation and properties of magnetic Fe₃O₄–chitosan nanoparticles. *Journal of alloys and compounds*, 466, 451–456.
- Liu, C., & Bai, R. (2005). Preparation of chitosan/cellulose acetate blend hollow fibers for adsorptive performance. *Journal of Membrane Science*, 267, 68–77.
- Liu, L., Won, Y., Cooke, P., Coffin, D., Fishman, M., Hicks, K., et al. (2004). Pectin/poly(lactide-co-glycolide) composite matrices for biomedical applications. *Biomaterials*, 25, 3201–3210. Science direct.
- Majid, S., Yuan, Y., Mishra, S., Haggard, W., & Burngardner, J. Effects of material property and heat treatment on nanomechanical properties of chitosan films. Wiley Periodicals in press.
- Nagahama, H., Maeda, H., Kashiki, T., Jayakumar, R., Furuie, T., & Tamura, H. (2009). Preparation and characterization of novel chitosan/gelatin membranes using chitosan hydrogen. *Carbohydrate polymers*, 76, 255–260.
- Niu, X., Feng, Q., Wang, M., Gui, X., & Zheng, Q. (2009). In vitro degradation and release behavior of porous poly(lactic acid) scaffolds containing chitosan microspheres as a carrier for BMP-s-derived synthetic peptide. *Polymer degradation and stability*, 94, 176–182.
- Perera, M., Ishiaku, U., & Ishak, Z. (2000). Thermal degradation of PVC/NBR and PVC/ENR binary blends and PVC/ENR50/NBR ternary blends studied by DMA and solid state NMR. *Polymer degradation and stability*, 68, 393–402.
- Roh, I., & Kwon, I. (2002). Fabrication of a pure porous chitosan bead matrix: influences of phase separation on the microstructure. *Journal of Biomaterials Science Polymer Edition*, 13, 769–782.
- Royall, P., Huang, C., Jai Tang, S., Duncan, J., Van-de-Velde, G., & Brown, M. (2005). The development of DMA for the detection of amorphous content in pharmaceutical powdered materials. *International journal of pharmaceutics*, 301, 181–191.
- Sakurai, K., Maegawa, T., & Takahashi, T. (2000). Glass transition temperature of chitosan and miscibility of chitosan/poly(N-vinyl pyrrolidone) blends. *Polymer*, 41, 7051–7056.
- Sánchez-Salcedo, S., Nieto, A., & Vallet-Regí, M. (2008). Hydroxyapatite/ β -tricalcium phosphate/agarose macroporous scaffolds for bone tissue engineering. *Chemical engineering journal*, 137, 62–71.
- Schiffman, J., Stulga L. & Schauer, C. Chitin and chitosan: transformations due to the electrospinning process. *Polymer engineering and science* in press.
- Sivalingam, G., & Madras, G. (2004). Thermal degradation of binary physical mixtures and copolymers of poly(ϵ -caprolactone), poly(D,L-lactide), poly(glycolide). *Polymer degradation and stability*, 84, 393–398.
- Sokker, H., Ghaffar, A., Gad, Y., & Aly, A. (2008). Synthesis and characterization of hydrogels based on grafted chitosan for the controlled drug release. *Carbohydrate polymers*, 75, 222–229.
- Souza, B., Cerqueira, M., Martins, J., Casariego, A., Teixeira, J. & Vicente, A. (2009). Influence of electric fields on the structure of chitosan edible coatings. *Food Hydrocolloids*.
- Sutton, D., Durand, R., Shuai, X., & Gao, J. (2006). Poly(D,L-lactide-co-glycolide)/poly(ethylenimine) blend matrix system for pH sensitive drug delivery. *Journal of Applied Polymer Science*, 100, 89–96.
- Thein-Han, W., & Misra, R. (2009). Biomimetic chitosan-nanohydroxyapatite composite scaffolds for bone tissue engineering. *Acta Biomaterialia*, 5, 1182–1197.
- Wan, Y., Wu, H., Yu, A., & Wen, D. (2006). Biodegradable polylactide/chitosan blend membranes. *Biomacromolecules*, 7, 1362–1372.
- Wan, Y., Fang, Y., Wu, H., & Cao, X. (2006). Porous polylactide/chitosan scaffolds for tissue engineering. *Journal of biomedical materials research*, 80, 776–789.
- Yuan, N., Lin, Y., Ho, M., Wang, D., Lai, J., & Hsieh, H. (2009). Effects of the cooling mode on the structure and strength of porous scaffolds made of chitosan, alginate, and carboxymethyl cellulose by the freeze-gelation method. *Carbohydrate polymers*, 78, 349–356.